Evaluation of Electric Field Measurement in Space Environment

Takanobu MURANAKA[1)], Hiroko O. UEDA[2),3)], Hideyuki USUI[4)] and Iku SHINOHARA[2)]

[1)]*JAXA's Engineering Digital Innovation (JEDI) Center, JAXA, 3-1-1 Yoshinodai, Sagamihara 229-8510, Japan*
[2)]*Institute of Space and Astronautical Science, JAXA, 3-1-1 Yoshinodai, Sagamihara 229-8510, Japan*
[3)]*Japan Science and Technology Agency, CREST, 3-1-1 Yoshinodai, Sagamihara 229-8510, Japan*
[4)]*Research Institute for Sustainable Humanosphere (RISH), Kyoto University, Gokasho, Uji 611-0011, Japan*

(Received: 13 September 2008 / Accepted: 14 November 2008)

Measuring the electric potential difference between the two points around a spacecraft is one of the simple ways to determine the electric field in space. Achieving the accurate measurement of the electric field, we need to consider spacecraft charging that affects the electric field around the spacecraft because the scale length of a spacecraft is much smaller than the Debye length in tenuous plasma environment. In addition to that, photoelectron emission from a spacecraft and probes is also considered to disturb the electric field. Evaluating accurate electric field measurement on-board spacecraft, we had numerically studied the electric potential around a spacecraft under tenuous plasma environment including photoelectron emission by using a three-dimensional electrostatic full Particle-In-Cell code. In this paper, first, fundamental functions that are required for the computation were validated in Geosynchronous Orbit environments by comparing with the thick-sheath limit theory. Second, the floating potential of a spacecraft model with photoelectron emission in Geosynchronous Orbit was computed to examine the effects of photoelectron emission to the electric potential around the spacecraft. The dependence of the floating potential on the photoelectron temperature was shown in the simulation.

Keywords: Electric field measurement in space, Tenuous plasma environment, Photoelectron emission, Spacecraft-plasma interactions, 3D Particle-In-Cell code

1. Introduction

Measurement of the electric field on-board spacecraft has the difficulties because of its smallness, typically less than a few mV/m. On one hand, spacecraft itself easily has the artificial electric field of the order of 100 mV/m generated by spacecraft charging. The simple solution of this intrinsic problem is to measure the potential difference between the two points sufficiently apart from the spacecraft. In tenuous plasma environment like Geosynchronous Orbit (GEO), the Debye length is estimated to be more than several tens of meters that is much greater than the scale length of a spacecraft. So the measurement system requires long booms in order to locate the probe sensors outside the sheath region around the spacecraft. Considering appropriate configuration for the measurement system applying this concept, it is of importance to estimate the spatial distribution of plasmas around the spacecraft that is self-consistently determined by the floating potential of the spacecraft and the plasmas around it.

In GEO environment, the eclipse floating potential of the spacecraft is of the order of negative kV, whereas, in sunlight, the spacecraft has the positive floating potential because of the photoelectron current from the sunlit surface which amounts to about ten times greater than the ambient electron current. Furthermore, in very low-density plasma environment like magnetosphere, it is considered that the temperature of the photoelectron emission plays an important role to determine the magnitude of the spacecraft potential [1].

In order to perform quantitative analyses of these issues between spacecraft and space environment plasmas, we have developed a three-dimensional electrostatic full Particle-In-Cell [2] code [3] based on the high-performance computation code [4]. In the numerical space, we can simulate tenuous plasma environment including photoelectron emission (PEE) from the sunlit surface of a spacecraft. Because the algorithm adopted in the code has no robustness, we can compute transitional phenomena such as sheath formation including PEE, and then obtain the saturation value of the floating potential of the spacecraft and spatial distribution of the electric potential around it as a result of steady state solution of the computation. In the algorithm, the spacecraft

muranaka.takanobu@jaxa.jp

charging analysis technique is referred that is employed in the MUSCAT [5-7] algorithm, a spacecraft charging analysis software made in Japan.

In this paper, we computed the interactions between single conductor and environment plasmas as the first step of the computation of the measurement system. In the computations, we neglected the existence of the geomagnetic field because the gyro radii of ambient electrons and ions were much greater than the spacecraft scale in GEO environment (e.g. about 300 m for 100 eV thermal electrons). First, we validate the code for its fundamental functions such as current collection and determination of the electric field. Second, the computations with PEE using the same model are shown. The effect of the photoelectron temperature on the floating potential of the spacecraft and potential structure around that is also discussed.

2. Floating potential of a Spacecraft in GEO environment

Floating potential of a spacecraft relative to the space potential is generally defined that the net current to the spacecraft body is zero at the potential in the space environment. We first performed the computation in order to obtain the saturate floating potential for a conductor model under only the ambient plasma environment at GEO. In GEO environment, as mentioned before, the Debye length is greater than several tens of meters, and that is much greater than the scale length of a spacecraft. Thus the current collection is described by the thick-sheath limit theory, that is, Orbital Motion Limited (OML) theory.

Table 1 shows the calculation parameters used in this simulation. For a preliminary simulation in GEO environment, we selected the plasma density of the order of 10^6 m^{-3} and the temperature of 100 eV to decrease the Debye length as possible. That reduced the computational resources and time. The spacecraft model was a conductor cube of its one side 2.0 m.

The temporal profile of the body potential is shown in Fig. 1. The body potential saturates at -225 V in 0.018 seconds. Because we only consider primary isotropic Maxwellian electrons and ions for this case, the net current density from the OML theory for an object with a spacecraft potential $V_s < 0$, is given by [8]

$$j_{net}(V_s) = j_{0e}\exp(-e|V_s|/kT_e) - j_{0i}(1+e|V_s|/kT_i), \quad (1)$$

where

$$j_{0e,i} = en_{e,i}\sqrt{kT_{e,i}/2\pi m_{e,i}}\,. \quad (2)$$

Table 1. Computation Parameters for GEO Environment.

plasma density, n [m^{-3}]	5×10^6
plasma temperature, T [eV]	100
mi/me (H)	1836
Debye length [m]	33
numerical domain	64x64x64
object size	2x2x2
dx [m]	1.0
dt [s]	4.2×10^{-8}

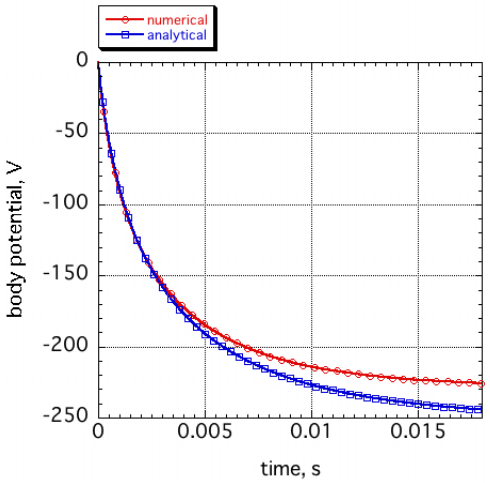

Fig. 1 Temporal profile of the floating potential; numerical result for a conductive cube and analytical one for a conductive sphere obtained by integrating the current balance equation by 4-th order Runge-Kutta method.

The saturation value of the potential is given by

$$V_s = -\frac{kT_e}{e}\ln\left[\sqrt{\frac{T_i}{T_e}\frac{m_e}{m_i}}(1-eV_s/kT_i)\right]. \quad (3)$$

For $(mi/me)^{1/2}$=42.8, kT_e/e=100 eV and kT_i/e=100 eV, Eq. (3) gives the saturated potential Vs=-250 V.

The time scale to reach the steady state is given by integrating the following equation

$$C_{SC}\frac{dV_s}{dt} = j_{net}A\,, \quad (4)$$

where C_{SC} and A are the capacitance of the body surface obtained by the capacity matrix method [9], the body surface area, respectively. We approximate the body as a sphere of radius R. Then, we have

$$\frac{dV_s}{dt} = \frac{R}{\varepsilon_o}j_{net}\,. \quad (5)$$

Substituting Eq. (1) into the above, we obtain

$$\frac{dV_s}{dt} = \frac{R}{\varepsilon_o}\left[j_{0e}\exp(eV_s/kT_e) - j_{0i}(1-eV_s/kT_i)\right]. \quad (6)$$

We integrate this equation using the 4th-order Runge-Kutta method for R=1.0 m and plot the temporal variation of V_s in Fig. 1. The temporal profile calculated from the OML theory and the time scale agree well with the temporal profile calculated from this code. The saturation value from the computation is slightly higher than the analytical one.

3. Photoelectron Emission in GEO Environment

In order to simulate the real space environment in sunlight in addition to shadow environment as possible as we can, we have developed the function for photoelectron emission (PEE). Modeling the PEE in the simulation, the photoelectron temperature is important to determine the floating potential of the spacecraft in tenuous plasma environment as mentioned before [1].

3.1. Definition of the PEE function in the code

Photoelectrons are defined as emitting electrons from the sunlit surface of a spacecraft. We consider the distribution of the electrons as uniform in space on the sunlit surface, and as single Maxwellian in velocity space with cosine emission in the simulation. The total number of photoelectrons emitting in unit computation time dt from the square of unit computation length dx*dx is determined by the known possible photoelectron current density j_{ph0} at 1AU, which depends on the surface material,

$$N_{ph} = (j_{ph0}\cos\theta / e)\cdot dt \cdot dx^2 = (j_{ph} / e)\cdot dt \cdot dx^2 , \quad (7)$$

where θ is the incidence angle of the solar flux to the spacecraft surface.

As an example of the simulation with PEE in GEO environment, Fig. 2 shows temporal profile of the floating potential with photoelectron and ambient electron currents. The saturation value of the floating potential is about 0.15 V, although that without PEE -230 V as shown in Fig. 1.

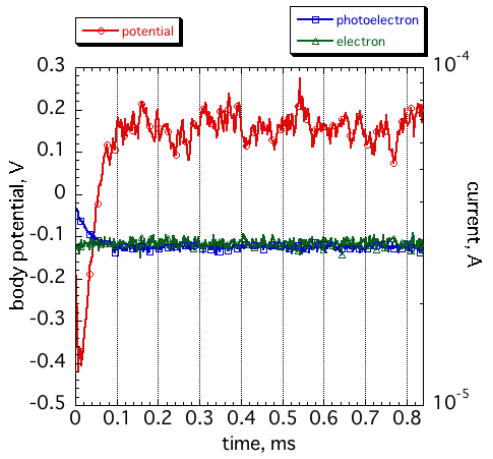

Fig. 2 Temporal profile of the floating potential, ambient electron current and photoelectron current.

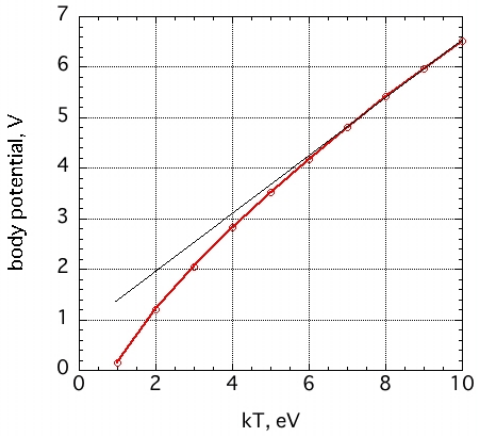

Fig. 3 The saturation potential of the conductor cube vs photoelectron temperature plotted by the red solid line with open circles. The black solid line shows the linear line fitting the numerical results over 6 eV.

3.2. Dependence of floating potential on photoelectron temperature

Using the developed PEE function mentioned above, we examined the dependence of the floating potential on the photoelectron temperature including the space charge effect of them. We performed the computations for photoelectron temperature kT_{ph}/e, from 1.0 to 10.0 eV under the fixed photoelectron current density of 10 μA/m^2. It was already studied in magnetosphere by the GEOTAIL spacecraft observation, for example, that the net current of photoelectron [10] and the temperature model that well represents the observation data [1]. (Observation data in ref. [1] and [10] were obtained during the period from 1992 to 1998, not averaged data during the 11-year solar cycle.) We adopted single temperature PEE model mentioned before for simplicity.

Figure 3 shows the floating potential of the conductor cube as a function of the photoelectron temperature. The red solid line with open circles shows the computation result.

Here, the net current for Vs > 0 is obtained by the current balance between ambient electrons and ions, and photoelectrons as follows [8],

$$j_{net}(V_s) = j_{0e}(1+eV_s / kT_e) - j_{0i}\exp(-eV_s / kT_i) - j_{ph0}\exp(-eV_s / kT_{ph})(1+eV_s / kT_{ph}) . \quad (8)$$

We have the solution from j_{net}=0 for $V_s > 0$, considering $kT_{ph} \ll kT_e$ [8],

$$V_s \approx \frac{kT_{ph}}{e}\ln[j_{ph0}(1+eV_s / kT_{ph}) / j_{oe}] . \quad (9)$$

From this equation, it can be supposed that $V_s \sim kT_{ph}$ /e.

The black solid line in Fig. 3 shows the linear line fitting the numerical results over 6 eV. The floating potential shows linearity in photoelectron temperature in this region. On the other hand, for V_s < 6 eV, as the photoelectron temperature becomes low, the floating potential becomes smaller than the linear value plotted in Fig. 3. For kT_{ph}/e = 1.0 eV, V_s = 0.15 V, that is almost one-order smaller than the expected order of the floating potential by Eq. (9).

Figure 4 shows the spatial profiles of the electric potential on the zx-plane for kT_{ph}/e = 1.0, 3.0 and 10.0 eV. Photoelectrons were emitted from the positive x-plane on the cube in the simulations. In case of kT_{ph}/e = 1.0 eV, it is recognized from Fig. 4-a that the electric potential near the surface where photoelectrons leave is lower than the space potential around because the diffusion speed of the photoelectrons is low to escape from the surface. The space charge of the photoelectrons themselves forms potential barrier to the emitting photoelectrons with lower kinetic energy than the potential depth. We recognized similar potential barrier in front of the emission surface for kT_{ph}/e from 1.0 eV to 4.0 eV, and the depth of the potential barrier decreased as the photoelectron temperature increased, as shown in Fig. 4-b. On the other hand, for kT_{ph}/e from 5.0 eV to 10.0 eV, such potential barrier is not significantly recognized. In these cases, the photoelectrons are considered that they have enough diffusion speed from the emission surface. Figure 4-c shows the profile of the electric potential not forming the potential barrier for kT_{ph}/e = 10. 0 eV.

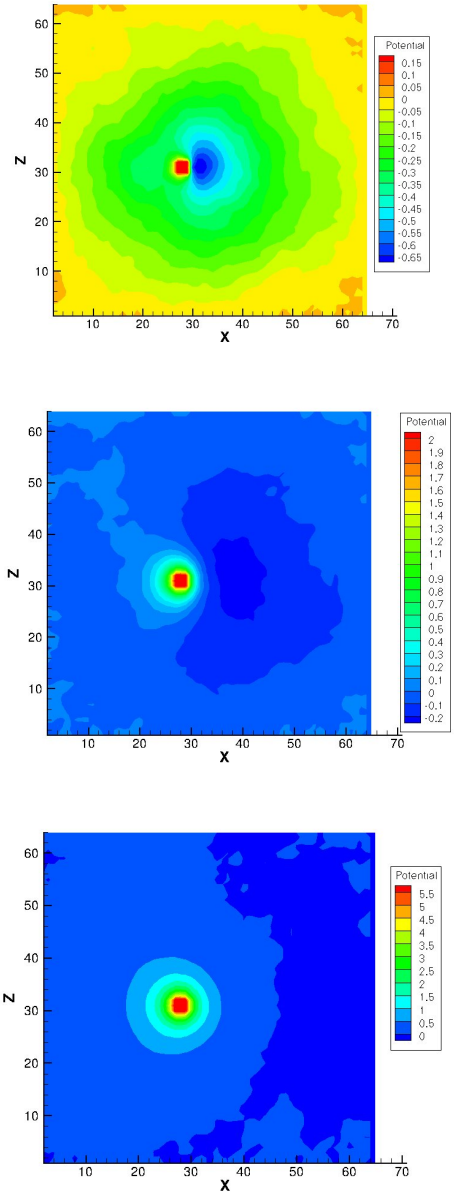

Fig. 4 Spatial distributions of the electric potential with photoelectron emission at 0.84 ms, (a) in the case for kT_{ph}/e=1.0eV (above), (b) kT_{ph}/e =3.0eV (middle) and (c) kT_{ph}/e =10.0 eV (below), respectively.

Considering these results, the space charge of the photoelectrons near the emission surface could form the potential barrier to the photoelectrons, which result in the increase of the return current of them. In the end, that decreases the net current onto a spacecraft. The temperature of the photoelectrons is of importance to determine the electric potential profile around the spacecraft and the current collection onto it.

4. Conclusion

We have developed a three-dimension electrostatic full Particle-In-Cell code to analyze the spacecraft-plasma interactions. In order to evaluate the electric field measurement in real environment as possible, we have extended the code by including the photoelectron emission that is crucial for spacecraft charging under the tenuous ambient plasma environment. Fundamental physical functions are validated such as current collection, computation of the electric potential including the floating potential of a conductor model.

We first evaluated these functions in GEO environment under the ambient plasma environment by comparing the thick-sheath limit theory, i.e., OML theory. The numerical and theoretical results were in good agreement about the saturation value of the floating potential and the time constant for the saturation.

Next, in GEO environment, dependence of the floating potential on the photoelectron temperature was numerically studied as the first step to the evaluation of electric field measurement on-board spacecraft. The result showed that the photoelectrons with low energy could form the potential barrier near

the emission surface. That could increase the return current of the photoelectrons and the diffusion of photoelectrons toward the spacecraft. These results show the importance of the model of the photoelectron temperature adopted in the simulation.

As a future work, we will install more than two conductors into the numerical space, and simulate the probe for potential measurement on-board spacecraft, and the electric circuit model. We will also study the appropriate photoelectron temperature model by comparing the observation data.

Acknowledgement

The computation in this work was performed at the Information Technology Center in Nagoya University collaborating with the Solar-Terrestrial Environment Laboratory. The computation was also performed with the JAXA Supercomputer System (JSS).

[1] Ishisaka, K., "Analysis of GEOTAIL Spacecraft Potentials and Its Application to the Magnetospheric Plasma Diagnostic," Ph. D thesis, Mar. 2000.

[2] Birdsall, C. K., and Langdon, A. B, *Plasma Physics via Computer Simulation*, McGraw-Hill, New York, 1985.

[3] Muranaka, T., Ueda, H. O., Usui, H., and Shinohara, I., "Evaluation of Electric Field Probe On-board Spacecraft Using a 3D Full PIC Simulation, " *Proc. 26th International Symposium on Space Technology and Science*, Hamamatsu, Japan, 1-8 June, 2008.

[4] Usui, H., Miyake, Y., Okada, M., Omura, Y., Sugiyama, T., Murata, K. T., Matsuoka, D., Ueda, H. O., "Development and Application of Geospace Environment Simulator for the Analysis of Spacecraft-Plasma Interactions," IEEE Transactions on plasma science, Volume 34, Issue 5, part2, pp2094- 2102, Oct. 2006.

[5] Hatta, S., Muranaka, T., Hosoda, S., Kim, J., Cho, M., Ueda, H. O., Koga, K., and Goka, T., "Progress of Multi-Utility Spacecraft Charging Analysis Tool (MUSCAT) and its Evolution for Space Exploration," IAC-06-D5.2.08, *Proc. 57th International Astronautical Congress*, Valencia, Spain, October 2006.

[6] Muranaka, T., Hatta, S., Kim, J., Hosoda, S., Ikeda, K., Cho, M., Ueda, H. O., Koga, K., and Goka, T., "Final Version of Multi-Utility Spacecraft Charging Analysis Tool (MUSCAT), " *Proc. 10th Spacecraft Charging Technology Conf.*, Biarritz, France, 18-21 June, 2007.

[7] Hosoda, S., Muranaka, T., Kim, J., Hatta, S., Kurahara, N., Cho, M., Ueda, H. O., Koga, K., Goka, T., and Kuninaka, H., "Verification of Multi-Utility Spacecraft Charging Analysis Tool (MUSCAT) via Laboratory Test," *Proc. 10th Spacecraft Charging Technology Conf.*, Biarritz, France, 18-21 June, 2007.

[8] Hastings, D., and Garrett, H., *Spacecraft-Environment Interactions*, Cambridge Atmospheric and Space Science Series, Cambridge University Press, UK, 1996.

[9] Hockney, R. W., and Eastwood, J. W., Computer Simulation Using Particles, Institute of Physics Publishing, Bristol and Philadelphia, 1988.

[10] Nakagawa, T., Ishii, T., Tsuruda, K., Hayakawa, H., and Mukai, T., "Net Current Density of Photoelectrons Emitted from the Surface of the GEOTAIL spacecraft," Earth, Planets and Space, vol. 52, pp283-292, 2000.